Modelling Flow Phenomena in Time Dependent Store Release from Transonic Aircraft

D A MacLucas and I M A Gledhill

Defence, Peace, Safety and Security Unit,
CSIR, PO Box 395, Pretoria 0001 South Africa

E-mail: igledhil@csir.co.za

Abstract. Computational Fluid Dynamics is routinely used in clearance of stores for carriage and release from aircraft in the transonic range of flight. A well-known validation case is modelled in this study, for which aerodynamic loads have been compared with wind tunnel experimental data by other authors. In this study, having validated the numerical model, we apply more recent methodologies from flow dynamics to study the detailed flow field in the region of the store fins.

1. Introduction

In the Mach number range between 0.8 and 1.2, aerodynamic loads on aircraft and launch vehicles are very sensitive to the presence of shocks. This is of particular relevance in the carriage of stores on transonic aircraft such as the South African Air Force SAAB Gripen JAS-39C and D multi-role fighters, and the BAES Hawk 120 Lead-in Fighter Trainer. Notably, where store fins are closely positioned to the supporting pylon, choked flow may occur, leading to a low-pressure footprint on the upper aft surface of the store. The consequent significant nose-down pitch on release may result in contact between the store and the aircraft, risking the aircraft and pilot in the collision. Explosive Release Units (ERUs) are fitted in such cases. All stores must be cleared for carriage and release before flight test commences.

During the weapons integration and clearance phase, computational calculations and wind tunnel tests are conducted. While numerical models in the subsonic and supersonic ranges rely on a range of assumptions and can be executed relatively fast, transonic models are very sensitive to geometry and are computationally demanding.

Computational Fluid Dynamics (CFD) is complementary to wind tunnel test and flight test. CFD is routinely used for certification among NATO (North Atlantic Treaty Organization) countries [1], and is increasingly used for aerodynamic characterization, aeroelastic studies, risk reduction, and optimization. CFD is used in conjunction with faster methods such as panel methods (Green's function calculations), full potential models with closely coupled boundary layer solvers, and empirical methods, but is the only methodology providing capture of shocks and viscous phenomena through the complete transonic range. In carriage configurations, solution of the Navier-Stokes equations and a selected turbulence model is required. In time-accurate release cases, the inviscid Euler equations are usually a good enough approximation, and a six-degree-of-freedom (6DOF) trajectory solution with fully time-accurate flow is obtained. In contrast, Captive Trajectory Systems (CTS) in transonic wind tunnels must rely on a quasi-steady approximation, in which steady flow at sample points along the store trajectory is used to derive loads.

Validation of directly relevant cases in CFD is a rigorous requirement. The case of a double-ogive finned store dropped from a pylon beneath a delta wing has been studied experimentally [2] [3] and is a much-referenced case [4] in which aerodynamic loads on the store and translational and rotational displacements are used for validation. In this paper, we use this public domain case to study the detailed flow field and its time-dependence in the interference region. A full time-accurate inviscid computation of the case is performed in conjunctions with a 6DOF solver with the aim of predicting the store trajectory and capturing the transient flow phenomena.

The wing is a clipped delta wing, based on the NACA 64A010 section, with a 45° leading edge sweep angle supported by a centreline sting. The store is a tangent ogive forebody and similar afterbody with a cylindrical centrebody, and truncated NACA0008 fins with a 60° leading edge sweep. The store has a full scale mass of 907kg. The afterbody is truncated to accommodate the sting support of the CTS. No turbulence tripping was used. Full scale geometry, in which the mean aerodynamic chord of the wing is 4.32 m, was scaled down to 5% for the wind tunnel test. The experimental Reynolds number was 2.4 x 10^6 per foot, which corresponds to 34 million based on the mean aerodynamic chord in the full scale model. The experimental tests of interest were conducted at the Arnold Engineering Development Center (AEDC) [3] at angle of attack α=0° and Mach number M = 0.95. In the carriage position the separation distance of the store from the pylon was 0.070 inches. Data corrections may be found in the original report. The test case was conducted at a static temperature T = 236.707 K and static pressure p ~ 36042 Pa.

2. Methodology

Geometry was modelled at full scale. The simulation axes are illustrated below in Figure 1a.The flight axis and store-fixed axes are illustrated below in Figure 1b. The *x* axis is oriented in the direction of flow, the *y* axis from the centreline to the wing tip, and the *z* axis in the upwards direction in flight. The store and force moment coefficients are computed about the store body-fixed axis. A decision is required on whether to model the store sting or not. In this case, the sting is not modelled to match the flight condition as opposed to the wind tunnel condition.

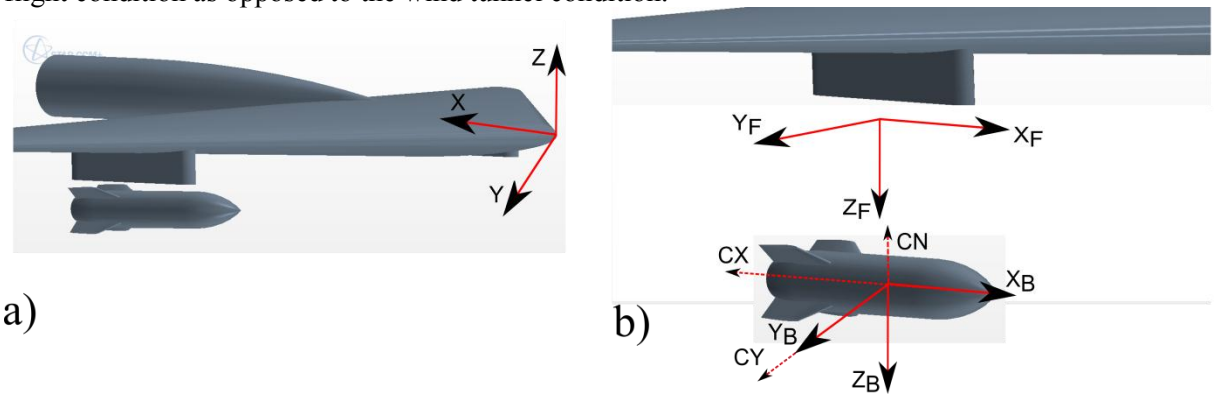

Figure 1: Axis systems. a) Simulation axes b) Flight axis set at the store centre of gravity in the carriage position below the pylon. Body-fixed axis fixed to the store centre of gravity. Positive sense for the normal force coefficient CN, side force CY and axial force coefficient CX illustrated.

A coupled density-based solver included in the CFD package Star-CCM+ v8.04 was used. Spatial discretisation is 2nd order upwind in order to capture shock and discontinuities adequately, with solution by a coupled implicit solver. Inviscid flux discretization is the AUSM+ flux vector splitting scheme [5]. Since dispersive numerical effects degrade the solution at shocks in this scheme, the Venkatakrishnan gradient reconstruction limiter [6] is applied. A 6DOF model was included to solve for the store translation and rotation about all three axes during release. Far field boundary conditions

are set as follows relative to the simulation axes: 90 m from the wing upstream and downstream; 50 m in the cross-flow direction and 100m in the *z* direction.

A grid of approximately 9 million hexadedral-dominant cells was used to discretize the computational domain for the carriage model. In order to accommodate the 6DOF motion of the store, overset, or Chimera, grids were constructed. These allow motion of an independently-generated store grid through a background grid attached to the wing. Grids are illustrated in Figure 2 below. Refinement zones were also generated for both the parent and the release corridor. These assist with increasing the grid resolution in these areas of interest without significantly increasing the overall cell count. The grid size along the boundary of the overset region was matched to the uniform grid size spacing in the release corridor as required by the overset method [7,8]. A distance-weighted interpolation scheme was used to interpolate between the background and overset grids.

The CFL (Courant-Friedrichs-Lewy) number, which determines stability of the method and controls the speed of convergence, was set in carriage models at 50. The implicit integration scheme had 2nd order temporal accuracy where the time-step was set at 10μs. The number of inner iterations (pseudo-time steps) was set at 5. Convergence was monitored through both dependent variable residuals and the store force and moment coefficient histories. A settling time of 10 ms was included, prior to releasing the store, to ensure that the store force and moment coefficient values had sufficiently converged. Since the store ejectors were not modelled in this simulation, the 6DOF solver was initialised using the linear and angular velocities measured by the CTS at the end of the ejector stroke. Since the store has been constrained until the end of the carriage time, the aerodynamic forces on the store were introduced linearly over 5 ms once the carriage time had expired. The method is used to reduce any impact loads encountered by the store.

Due to the significant computation requirement of time-accurate simulations, the model was run over 6 days across 12 networked i7 quad-core machines (*i.e.* 48 cores). This resulted in 0.19 s of full-scale release time after the end of the nominal ejector stroke. This represents about a third of the remaining release time available from the experimental data. Further work will include a modelling running to 0.5 s, which is expected to take around 18 days. Much is to be said of managing the grid size since this has a significant effect on length of the simulation run. Providing the optimal grid resolution such that the necessary shock waves are captured whilst keeping the grid cell count low are critical elements in ensuring the simulation time is practical. In addition, selecting the optimal number of the quad core machines requires a thorough benchmarking exercise which is planned for future work.

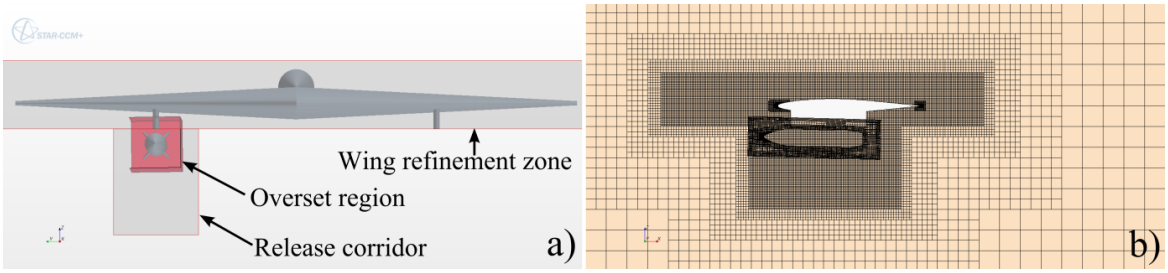

Figure 2 a) Background and parent grids. b) Mesh cross-section through the centre line of right wing's pylon. Note the parent and release corridor increased grid resolution in the refinement zones. Store is orientated to match attitude recorded by the CTS in the wind tunnel experiment.

3. Results

Figure 3 below illustrates the variation of the store force coefficients during carriage, including the force ramping time. This plot clearly indicates the requirements for the establishment of flow in the carriage configuration, since the forces take nearly 1000 time steps to reach approximately steady-state behaviour. By the end of this time, the side force coefficient CY is close to, but has not reached, a steady value, and therefore, in future models, this time will be at least doubled. Spikes are observed in

the normal force coefficient CN, and the side force coefficient CY, at the start of the ramp time. This was not expected, since the ramping of the force was used to reduce impact loading on the store. However, these spikes dissipate quickly and do not appear to have a significant on the results that follow.

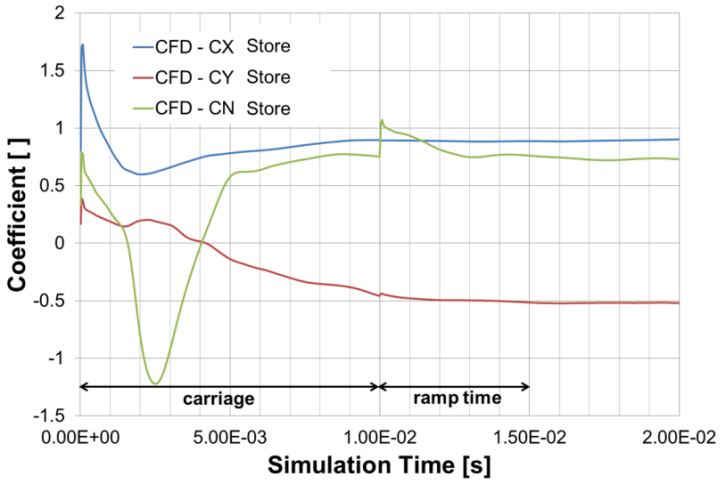

Figure 3 Store force coefficients variation during carriage and force ramping periods.

Figure 4 below shows the comparison between the trajectories recorded by the CTS and the computational result. The correlation between experiment and computation is excellent. It is noted that there are larger discrepancies for the *z* component of the trajectory. It is quite likely that this is a result of a small difference in the position of the store measured by the CTS just after the firing of the ejectors, and that used to initialize the store position in the simulation. It is also important to note that though it is possible to initialize the linear and angular velocities of the store after the firing of the ejectors, it is not possible to do so accurately in the surrounding highly transient flow field. Further work will require the addition of the ejectors to capture the unsteady flow field correctly.

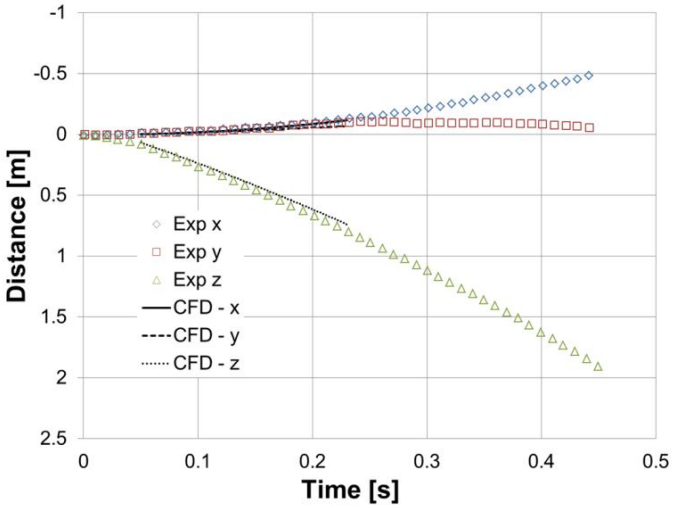

Figure 4 Computed store trajectory compared relative to pseudo-steady CTS wind tunnel results.

Figure 5 below illustrates the store force and moment coefficient histories plotted against the experimental results. Figure 5a illustrates a good correlation between the experimental and computational results despite the initial spike in the force coefficients due to the ramping (as described above). Interestingly, the axial force coefficient found in the simulations is in good agreement with the

experimental value despite the simulation being inviscid in nature, indicating that wave and form drag, rather than viscous drag, may be the primary effects. Since the sting is not included in the simulation, it is expected that the drag force would be higher than the wind tunnel configuration with the sting. This is most likely since the arrangement in the simulation results in a larger wake region, thereby increasing drag. Should the sting have been included in the simulation the axial force coefficient should be expected to be lower than the experimental results since viscous forces are not accounted for in the current simulation scheme.

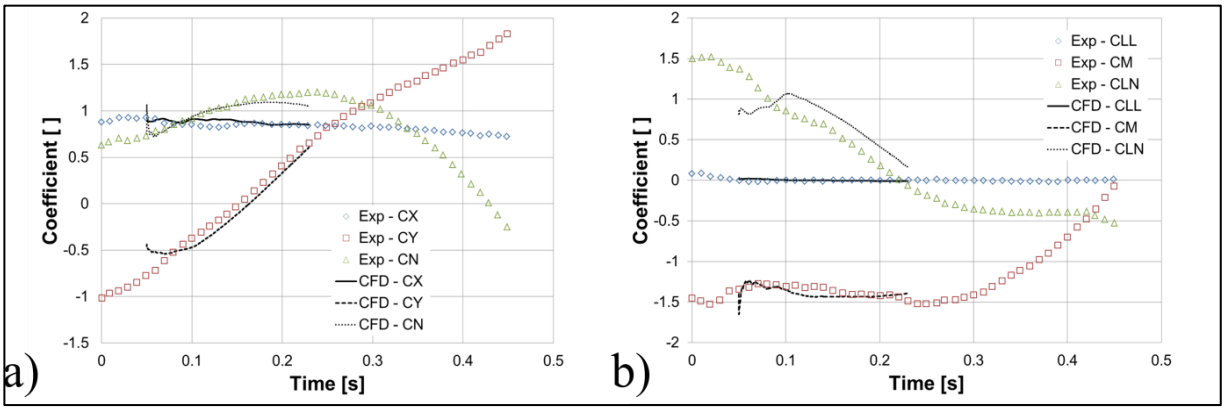

Figure 5 Store force and moment comparison with the wind tunnel results. a) Store force coefficient history, b) Store moment coefficient history.

The moment coefficients histories are illustrated above in Figure 5b. These also show relatively good agreement except for the yawing coefficient CLN. The computational results exhibit a nearly constant offset from the experimental results. This again may be a property of the initialization. Despite the flow outboard from the wing centre line of the delta wing, the rolling moment coefficient of the store is nearly zero, as seen in both sets of results. Agreement with the pitching moment CM is relatively good. This is a key indicator for flight clearance since a strong negative pitching moment, as seen in this case, could result in the rear of the store colliding with the parent as the store pitches downward. This curve illustrates the necessity for ejectors to displace the store from the parent during release.

It is important to note that in this work a comparison is made between pseudo-steady results from the wind tunnel CTS experiment, and a fully time-accurate unsteady computational approach. Therefore, full agreement between the two, since the experiment, with time steps of the order of 200 μs, does not capture the unsteady flow field, as calculated computationally (and observed in test flight). Therefore, differences between the two sets of results should be expected.

Figure 6 below illustrates the complex flow field developed on the underside of the wing of the parent during release of the store. Two shocks, L_1 and L_2, develop on the fore sections of the pylon. On the aft section of the pylon two additional shocks P are found on either side of the aft sections of the pylon. Interestingly, the shock P on the outboard section of the pylon is preceded by an expansion (see red contour adjacent to P). Note that there is a mutual interference between the store and pylon where numerous shocks are visible on the underside of the store. These shocks impinge on the fins of the store and they have significant effects on the yawing and pitching moment of the store during the early stages of release. Figure 6 also illustrates a wake region developing behind the pylon which interacts with the wing trailing edge shock W. The transient wake region tends to disrupt the shape and magnitude of the wing shock W. In addition, it is found that there is a transient interaction between the aft pylon shocks P and this wake region. Further work is required to quantify this transient behaviour on the loading the store experiences and establish whether it ultimately affects the store's trajectory.

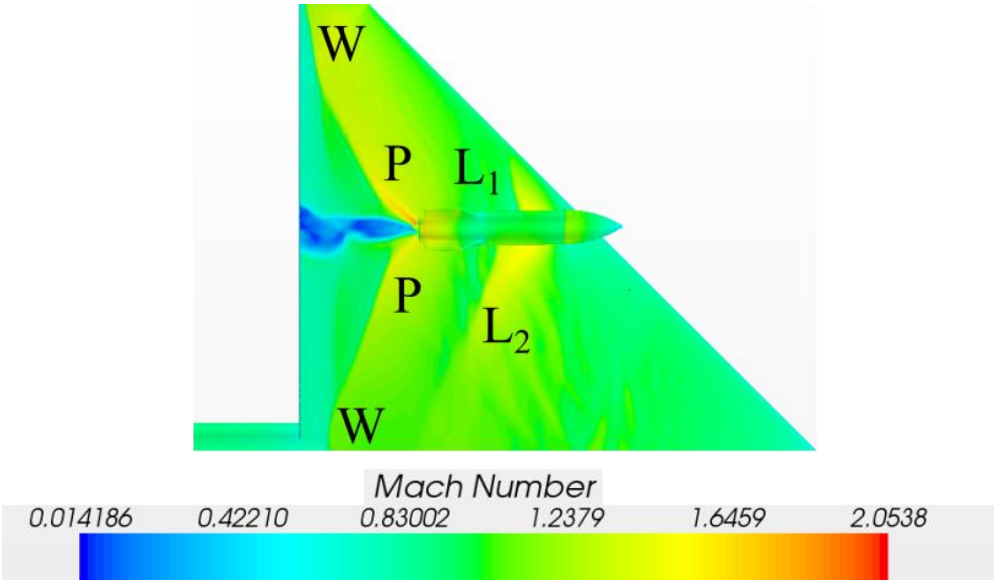

Figure 6 Contours of Mach number for the underside of the wing and the store during release stage.

4. Conclusions

Preceding simulations to the current work of the parent alone indicated that the flow beneath the wing is highly transient thereby necessitating the need for the current work of performing time-accurate time modelling of release. The time-accurate 6DOF release of a store from a parent was successfully conducted in Star-CCM+. A good level of agreement between computation and experiment was observed for both the trajectory and the store loads. However, there were deficiencies in the method which require further work. This includes modelling the ejectors and finding methods to minimize the total grid count while maximising the resolution of the shocks in the system which have significant effects on the store loads. The potential of adaptive gridding will be explored in future work since it would be ideal for this case. In addition, a benchmarking exercise is necessary to minimise the run time of the simulation on a cluster of machines. Further analysis of the flow field under the wing is also necessary in order to quantify the effect of these transient flow fields on the trajectory of the store.

References

[1] Cenko A 1992 Store separation lessons learned during the last 30 years. In *27th Int. Conf. of the Aeronautical Sciences*

[2] Fox J H 2000 Generic wing, pylon, and moving finned store *Technical report, Defence Technical Information Center ADP010735*

[3] Heim R 1991 CFD wing/pylon/finned store mutual interference wind tunnel eperiment *Technical report Arnold Engineering Development Center*

[4] Lijewski L E and Suhs N E 1994 Time-accurate computational fluid dynamics approach to transonic store separation trajectory prediction *J. Aircraft* **31** 886–891

[5] Liou M S 1996 A sequel to AUSM: AUSM+ *J. Comput. Phys.* **129** 364–382

[6] Venkatakrishnan V 1995 Convergence to steady state solutions of the euler equations on unstructured grids with limiters *J. Comput. Phys.* **118** 120–130

[7] Steger J L, Dougherty F C and Benek J A 1983 *A Chimera Grid Scheme, Advances of Grid Generation*, ed K N Ghia and U Ghia *American Society of Mechanical Engineers, ASME FED-5* (New York: ASME) 55-69

[8] Benek J A, Steger J L, Dougherty F C 1983 A Flexible Grid Embedding Technique with Applications to the Euler Equations *American Insitute of Aeronautics and Astronautics Paper 83-1944*